Inorganica Chimica Acta 498 (2019) 119174

Contents lists available at ScienceDirect

Inorganica Chimica Acta

journal homepage: www.elsevier.com/locate/ica

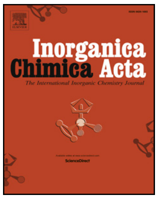

Mononuclear manganese(III) complex with a monodeprotonated *N*-(2-pyridylmethyl)iminodiisopropanol ligand: synthesis, crystal structure, and catalytic properties

Jihye Choi[a], Sojeong Lee[b], Ah Rim Jeong[a], Cheal Kim[b,*], Kil Sik Min[c,*]

[a] *Department of Chemistry, Kyungpook National University, Daegu 41566, Republic of Korea*
[b] *Department of Fine Chemistry, Seoul National University of Science and Technology, Seoul 01811, Republic of Korea*
[c] *Department of Chemistry Education, Kyungpook National University, Daegu 41566, Republic of Korea*

ARTICLE INFO

Keywords:
Manganese complex
N,O ligand
Azide ion
Crystal structure
Catalysis

ABSTRACT

The reaction of *N*-(2-pyridylmethyl)iminodiisopropanol (H_2pmidip), sodium azide, and manganese(II) salt in methanol leads to the isolation of a monomeric manganese complex of $[Mn(Hpmidip)(N_3)_2]\cdot CH_3OH$ (**1**). The structure of **1** has been verified by single crystal X-ray diffractometry. The manganese ion in **1** is bonded with one $Hpmidip^-$ as tetradentate and two azido ligands in *cis* position in which the manganese ion is displayed a distorted octahedral geometry. One of two hydroxyl groups in the coordinated $Hpmidip^-$ ligand is protonated, while the other one is deprotonated. The manganese ion is assigned as 3+ oxidation state that verified by bond lengths and bond valence sum. Furthermore, the complex reveals a dimeric structure by O—H···O hydrogen bonding interactions. **1** exhibited selective and effective catalytic properties for various olefins with moderate yields using *m*-CPBA (*meta*-chloroperoxybenzoic acid). The mechanistic studies of **1** for olefin epoxidation have been investigated by the Hammett study, the O—O bond cleavage of PPAA (peroxyphenylacetic acid) as a mechanistic probe, and competitive experiments of *cis*- and *trans*-2-octene.

1. Introduction

We are strongly concerned in the preparation of new transition metal compounds that show the catalytic olefin epoxidations [1]. A series of coordination compounds that exhibit the catalytic behaviors have been designed and prepared by using polynucleating ligands included functional groups, i.e., hydroxyl and amine moieties [2]. Furthermore, they have been shown interesting structures such as oxygen-bridged dinuclear and trinuclear complexes as well as unique magnetic properties, i.e., ferro- and antiferromagnetic couplings. We have recognized that the geometric structures of such compounds are also dependent on metal ions and anions. As such, these compounds have attracted much interest, because of their significant structures and magnetic properties including catalytic effects. In particular, incorporation of hydroxyl group into polynucleating ligands has been confirmed to be a useful method of controlling structure and oxidation state of coordination complexes [3]. Previously we have reported coordination complexes (Mn, Co) based on an N_3O-type tetradentate ligand (*N*,*N*–bis(2-pyridylmethyl)-2-aminoethanol, bpaeOH) [4]. Two manganese complexes $[Mn(bpaeOH)(NCS)_2]$ and $[Mn(bpaeO)(N_3)_2]$ are obtained as octahedral monomers, although they have different anions and oxidation states via bpaeOH or $bpaeO^-$, respectively. Unfortunately, both complexes did not show any catalytic effects for olefin epoxidations. Unlike the manganese species, two cobalt complexes in the same conditions are prepared as monomer $[Co(bpaeOH)(NCS)_2]$ and trimer $[Co_3(bpaeO)_2(NO_3)(N_3)_4](NO_3)$ depending on anions (NCS^- and $N_3{}^-$), respectively. The former is cobalt(II) oxidation state and displayed a non-catalytic effect, while the latter is Co^{3+}-Co^{2+}-Co^{3+} mixed-valence species and showed interesting catalytic properties.

Contrary to the above manganese species, other manganese coordination complexes with interesting catalytic oxidation properties have been reported [5]. For example, complex $[Mn^{II}Cl_2(pypz\text{-}H)_2]$ having *cis* fashion geometry showed 47% conversion and 60% selectivity for catalytic oxidation of styrene (pypz-H = 2-(3-pyrazolyl) pyridine) [5b]. As a Mn(III) complex, five-coordinate [Mn(bhbda)Cl] displayed 44.1% conversion and 82% selectivity for epoxidation of styrene using PhIO in acetonitrile (H_2bhbda = 1,4-bis(2-hydroxybenzyl)-1,4-diazepane) [5d]. That is, these manganese complexes are shown moderate conversions and selectivities in oxidation catalysis depending on multidentate ligands.

---

[*] Corresponding authors.
E-mail addresses: chealkim@seoultech.ac.kr (C. Kim), minks@knu.ac.kr (K.S. Min).

https://doi.org/10.1016/j.ica.2019.119174
Received 16 August 2019; Received in revised form 20 September 2019; Accepted 24 September 2019

Very recently, we have reported one trinuclear coordination complex, $[(pmidip)_2Co_3(CH_3COO)_4]$, based on deprotonated *N*-(2-pyridylmethyl)iminodiisopropanol ($pmidip^{2-}$) [2a]. In the cobalt trimer, two terminal Co(III) cations are connected to a central Co(II) cation through tetradentate $pmidip^{2-}$ and acetato ligands, which leads to a trinuclear Co^{3+}-Co^{2+}-Co^{3+} species. In this case, the oxidation state and the structure were very dependent on the $pmidip^{2-}$ ligand and the complex also showed efficient olefin epoxidations.

In order to explore the dependence of metal ion in the olefin epoxidations by using the N_2O_2-type ligand *N*-(2-pyridylmethyl)iminodiisopropanol ($H_2pmidip$) and azide ion, we have prepared a new manganese complex. The complex is a mononuclear manganese(III) complex and shows excellent catalytic effects, contrary to $[Mn(bpaeOH)(NCS)_2]$ and $[Mn(bpaeO)(N_3)_2]$ [4]. In this paper, we describe the synthesis, crystal structure, and catalytic activities of $[Mn(Hpmidip)(N_3)_2]\cdot CH_3OH$ (**1**).

2. Experimental section

All chemicals used in the synthesis were of reagent grade and used without further purification. *N*-(2-Pyridylmethyl)iminodiisopropanol ($H_2pmidip$) was prepared according to the literature procedure [2a]. Olefins, epoxides, 2-cyclohexen-1-ol, 2-cyclohexen-1-one, benzaldehyde, acetonitrile, dichloromethane, dodecane and *m*-CPBA (65%) were purchased from Aldrich Chemical Co. and were used without additional purification. Peroxyphenylacetic acid (PPAA) was synthesized according to the literature method [6]. Solvents used in inert-atmosphere reactions were dried and degassed using standard procedures. UV/Vis absorption spectra were recorded with a SCINCO S-2100 spectrophotometer and a Perkin Elmer model Lambda 2S UV/Vis spectrometer. Infrared spectra were recorded with a Thermo Fisher Scientific IR200 spectrophotometer ($\pm 1\ cm^{-1}$) using KBr disk. Elemental analyses were carried out using a Fisons/Carlo Erba EA1108 instrument in air. Flash column chromatography was performed with 230–400 mesh silica gel using wet-packing method. ^1H NMR spectra were recorded on a Varian AS400 (399.937 MHz for ^1H and 100.573 MHz for ^{13}C spectrometer) and chemical shifts were recorded in ppm. Analysis for epoxidation products was performed by using YL6500 gas chromatograph (Hewlett-Packard, HP-FFAP or DB-5).

2.1. Synthesis of $[Mn(Hpmidip)(N_3)_2]\cdot CH_3OH$ (1)

To a methanol solution (4 mL) of $Mn(NO_3)_2\cdot 4H_2O$ (50 mg, 0.2 mmol) was added dropwise a methanol solution (4 mL) of $H_2pmidip$ (45 mg, 0.2 mmol) and sodium azide (26 mg, 0.4 mmol). The color of the mixture solution became dark brown. The solution was stirred for 20 min at room temperature. Dark brown crystals of **1** were obtained by diffusion of diethyl ether into the dark brown solution for 3 days and were washed with diethyl ether and dried in air. Yield: 53 mg (66%). FT-IR (KBr, cm^{-1}): 3415, 3133(s, br), 3030, 2947, 2855, 2070, 2042, 1618. Anal Calcd for $C_{12}H_{19}MnN_8O_2$: C, 39.78; H, 5.29; N, 30.93; Found: C, 40.17; H, 5.65; N, 30.98.

2.2. Olefin epoxidations by m-CPBA with manganese catalyst 1

m-CPBA (1×10^{-1} mmol) was added to a mixture of manganese catalyst (2.8×10^{-3} mmol), substrate (3.5×10^{-2} mmol), and solvent ($MeCN/CH_2Cl_2$ (1/1), 1.0 mL). The mixture was shaken for 5 min at ambient temperature. Each reaction was analyzed by GC/mass with 10 µL aliquots taken periodically from the reaction solution. Product yields and conversions were quantified, compared to dodecane as an internal standard. All reactions were carried out three times, and the average of conversions and yields are represented. Product yields and conversions were based on substrate.

2.3. Competitive epoxidations of para-substituted styrenes and styrene for Hammett plot with manganese catalyst 1

m-CPBA (3×10^{-2} mmol) was added to a mixture of styrene (2×10^{-2} mmol) and *para*(X)-substituted styrene (2×10^{-2} mmol, X = $-CN$, $-Cl$, $-CH_3$, and $-OCH_3$), manganese catalyst (2.8×10^{-3} mmol), and solvent ($MeCN/CH_2Cl_2$ (1/1), 1.0 mL). The mixture was shaken for 5 min at ambient temperature. GC was used to measure the amounts of styrenes before and after reactions. The relative reactivities were analyzed with the following equation: $k_x/k_y = \log(X_f/X_i)/\log(Y_f/Y_i)$ where Y_i and Y_f are the initial and final concentration of styrene and X_i and X_f are the initial and final concentration of *para*-substituted styrenes [7].

2.4. Analysis of the O—O bond cleavage products generated from the oxidation reactions of substrates by PPAA with manganese catalyst 1

PPAA (4×10^{-2} mmol) was added to a mixture of manganese catalyst (2.8×10^{-3} mmol), substrate ($0–1.6 \times 10^{-1}$ mmol), and solvent ($MeCN/CH_2Cl_2$ (1/1), 1.0 mL). The mixture was shaken for 5 min at ambient temperature. Each reaction was analyzed by GC/mass with 10 µL aliquots taken periodically from the reaction solution. Product yields and conversions were quantified, compared to dodecane as an internal standard. All reactions were performed three times, and the average of conversions and yields are represented. Product yields and conversions were based on substrate or PPAA.

2.5. Competitive epoxidations of cis-2-octene and trans-2-octene by m-CPBA with manganese catalyst 1

m-CPBA (4×10^{-2} mmol) was added to a mixture of *trans*-2-octene (0.01–0.08 mmol), *cis*-2-octene (0.01–0.08 mmol), and manganese catalyst (2.8×10^{-3} mmol). The mixture was shaken for 5 min at ambient temperature. Each reaction was analyzed by GC/mass with 10 µL aliquots taken periodically from the reaction solution. Product yields and conversions were quantified, compared to dodecane as an internal standard. All reactions were performed three times, and the average of conversions and yields are represented. Product yields and conversions were based on substrate or *m*-CPBA.

2.6. X-ray crystallographic data collection and refinement

Single crystal of **1** was coated with paratone-*N* oil and the diffraction data measured at 100(2) K with synchrotron radiation (λ = 0.63000 Å) on an ADSC Quantum-210 detector at 2D SMC with a silicon (1 1 1) double crystal monochromator (DCM) at the Pohang Accelerator Laboratory, Korea. The ADSC Q210 ADX program [8] was used for data collection (detector distance is 63 mm, omega scan; Δω = 1°, exposure time is 1 *sec* per frame) and HKL3000sm (Ver. 703r) [9] was used for cell refinement, reduction and absorption correction. The crystal structure of **1** was solved by direct methods [10], and refined by full-matrix least-squares refinement using the SHELXL-2014 computer program [11]. The positions of all non-hydrogen atoms were refined with anisotropic displacement factors. All hydrogen atoms were placed using a riding model, and their positions were constrained relative to their parent atoms using the appropriate HFIX command in SHELXL-2014, except C8 (C8A and C8B). That is, C8 in **1** has large thermal disorder and thus is treated using PART command without fixing hydrogen atoms. The crystallographic data and the result of refinements are summarized in Table 1.

3. Results and discussion

3.1. Synthesis and characterization

The reaction of one equiv of *N*-(2-pyridylmethyl)

Table 1
Summary of the crystallographic data for **1**.

Compound	**1**
Empirical formula	$C_{13}H_{23}MnN_8O_3$
Formula weight	394.33
Crystal system	Monoclinic
Space group	$P2_1/n$
a (Å)	11.561(2)
b (Å)	11.771(2)
c (Å)	13.789(3)
α (°)	90
β (°)	108.59(3)
γ (°)	90
V (Å^3)	1778.5(7)
Z	4
d_{calc} (g cm^{-3})	1.473
λ (Å)	0.63000
T (K)	100(2)
μ (mm^{-1})	0.554
F(0 0 0)	824
Reflections collected	15,415
Independent reflections	4982
Reflections with $I > 2\sigma(I)$	3930
Goodness-of-fit on F^2	1.078
R_1[a] [$I > 2\sigma(I)$]	0.0588
wR_2[b] [$I > 2\sigma(I)$]	0.1707
CCDC no.	1915191

[a] $R_1 = \Sigma||F_o| - |F_c||/\Sigma|F_o|$.
[b] $wR_2 = [\Sigma w(F_o^2 - F_c^2)^2/\Sigma w(F_o^2)^2]^{1/2}$.

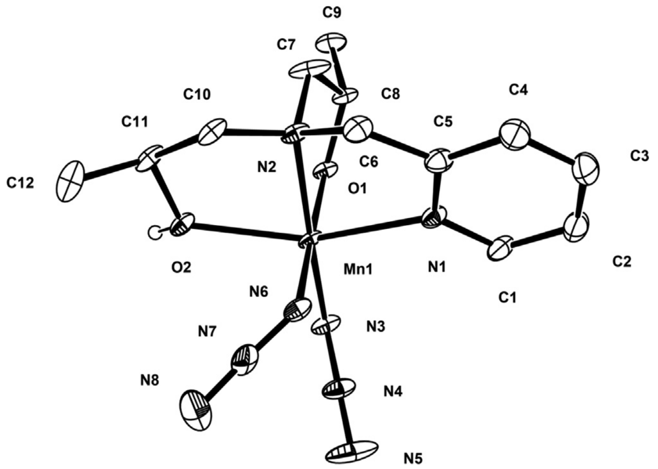

Fig. 1. Structure of $[Mn(Hpmidip)(N_3)_2]$ (**1**). The atoms are represented by 30% probable thermal ellipsoids. The hydrogen atom on the hydroxyl group is shown as small open circle; all other H-atoms are omitted for clarity.

Table 2
Selected bond distances (Å) and angles (°) for **1**.

Mn1—N1	2.249(2)	Mn1—N6	1.972(2)
Mn1—N2	2.131(2)	Mn1—O1	1.9060(17)
Mn1—N3	1.976(2)	Mn1—O2	2.2022(19)
N3—N4	1.192(3)	N6—N7	1.194(4)
N4—N5	1.147(3)	N7—N8	1.151(4)
N1—Mn1—N2	77.09(8)	N3—Mn1—O1	89.46(8)
N1—Mn1—N3	102.92(9)	N3—Mn1—O2	103.09(9)
N1—Mn1—N6	85.08(9)	N4—Mn1—O1	175.15(8)
N1—Mn1—O1	91.54(8)	N4—Mn1—O2	87.84(8)
N1—Mn1—O2	153.50(7)	O1—Mn1—O2	93.70(8)
N2—Mn1—N3	173.77(9)	Mn1—N3—N4	121.26(18)
N2—Mn1—N6	91.53(9)	Mn1—N6—N7	121.60(18)
N2—Mn1—O1	84.31(8)	N3—N4—N5	177.8(3)
N2—Mn1—O2	77.61(8)	N6—N7—N8	176.5(3)
N3—Mn1—N6	94.68(9)		

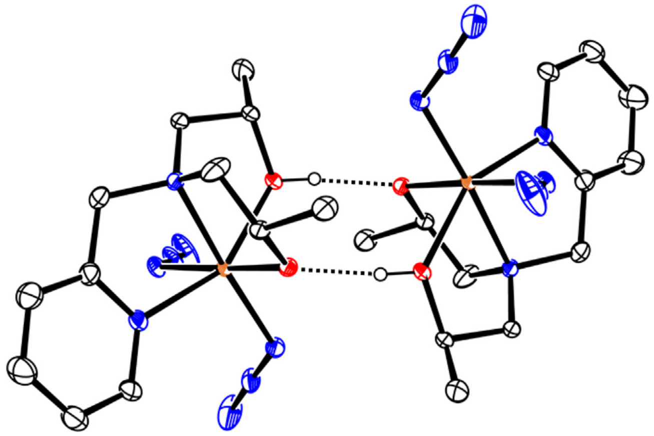

Fig. 2. Structure of $[Mn(Hpmidip)(N_3)_2]$ (**1**) showing hydrogen bonding interactions (dotted line).

Table 3
Olefin epoxidation by *m*-CPBA with **1** in CH_2Cl_2/MeCN (1/1).[a]

Entry	Substrate	Product	Manganese complex **1**[b]	
			Conversion (%)	Yield (%)
1	cyclopentene	epoxide	81.3 ± 0.9	34.6 ± 0.6
2	cycloheptene	epoxide	99.4 ± 0	44.4 ± 0.4
3	cyclooctene	epoxide	98.3 ± 0.1	39.4 ± 1.4
4	cyclohexene	epoxide	65.8 ± 4.0	49.6 ± 1.6
		2-cyclohexene-1-one		2.7 ± 0.2
		2-cyclohexene-1-ol		2.1 ± 0.1
5	1-hexene	epoxide	31.1 ± 4.0	7.7 ± 0.9
6	1-octene	epoxide	26.4 ± 1.2	5.6 ± 0.3
7	*cis*-2-hexene	*cis*-oxide	55.7 ± 0.5	39.7 ± 1.9
		trans-oxide		2.8 ± 0
8	*trans*-2-hexene	*trans*-oxide	41.1 ± 3.7	14.7 ± 2.0
9	*cis*-2-octene	*cis*-oxide	39.5 ± 0.9	31.5 ± 3.1
		trans-oxide		2.6 ± 0.7
10	*trans*-2-octene	*trans*-oxide	20.8 ± 1.0	13.5 ± 0
11	styrene	epoxide	58.3 ± 1.5	44.7 ± 2.9
		benzaldehyde		2.1 ± 4.8
		phenylacetaldehyde		8.3 ± 5.8
12	*cis*-stilbene	*cis*-stilbene oxide	69.3 ± 1.5	48.3 ± 0
		trans-stilbene oxide		5.5 ± 0.9
		benzaldehyde		4.6 ± 0.4
		2-phenylacetophenone		2.9 ± 0
13	*trans*-stilbene	*trans*-stilbene oxide	73.7 ± 0.1	37.8 ± 1.1
		benzaldehyde		4.4 ± 0
		2-phenylacetophenone		8.6 ± 7.0

[a] Reaction conditions: olefins (3.5×10^{-2} mmol), catalyst (2.8×10^{-3} mmol), *m*-CPBA (0.1 mmol), and solvent (1.0 mL, CH_2Cl_2/MeCN = 1:1).
[b] Based on substrate.

iminodiisopropanol (H_2pmidip), one equiv of $Mn(NO_3)_2 \cdot 4H_2O$, and two equiv of NaN_3 in methanol affords air stable $[Mn(Hpmidip)(N_3)_2] \cdot CH_3OH$ (**1**) in good yield (66%). Complex **1** is a mononuclear complex, which is obtained via tetradentate Hpmidip$^-$ and two azido ligands. Considered the charge of coordinated ligands (Hpmidip$^-$, $2\,N_3^-$), the oxidation state of **1** is 3+, in which it can be attributed to the oxidizing power of azide anions [4]. Complex **1** displays bonded Hpmidip$^-$ and azido ligands in infrared (IR) spectrum. For example, strong peaks at 2070 and 2042 cm^{-1} are displayed in which they are assigned to the monodentate azido ligands coordinated to manganese (III) ion [12]. The peaks of the C—H of Hpmidip$^-$ showed at 3030, 2947, and 2855 cm^{-1} and the peak of the O—H of Hpmidip$^-$ showed at 3133 cm^{-1}.

3.2. Description of structure of 1

Complex **1** crystallizes in the monoclinic $P2_1/n$ space group, and the

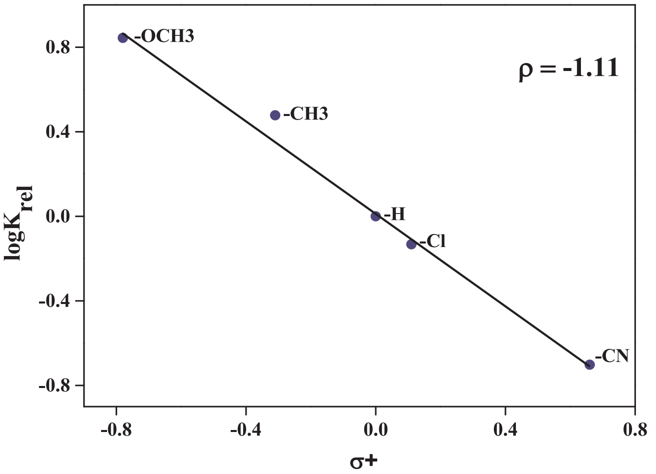

Fig. 3. Hammett plot for relative reactivities of *para*-substituted styrenes to styrene by manganese catalyst **1** with *m*-CPBA.

unit cell includes four mononuclear manganese complexes, and the ORTEP drawing of **1** is shown in Fig. 1. The selected bond lengths and angles are listed in Table 2. The manganese cation is bonded by two nitrogen atoms and two oxygen atoms of Hpmidip^- ligand and two nitrogen atoms of azido ligands. That is, the manganese ion adopts a distorted octahedral geometry with one Hpmidip^- ligand and two azido ligands. The manganese cation (Mn1) is coordinated to two oxygen atoms of Hpmidip^- ligand (av. Mn−O = 2.038(1) Å) and to two nitrogen atoms of Hpmidip^- ligand (av. $\text{Mn−N}_{\text{Hpmidip}}$ = 2.190(1) Å) and to two nitrogen atoms of azido ligands (av. Mn−⊖ N_{azido} = 1.974(1) Å). Interestingly, the H_2pmidip ligand in **1** is monodeprotonated to give Hpmidip^-. The bond distances Mn1−O1 and Mn1−O2 are 1.9060(17) and 2.2022(19) Å, respectively. From the difference of Mn−O bond distance (Δd = 0.2962 Å), we have noticed that the former is deprotonated and the latter is protonated. The average $\text{Mn−L}_{\text{Hpmidip}}$ bond distance is 2.106(1) Å and the $\text{Mn−N}_{\text{azido}}$ bond distnaces are 1.972(2) and 1.976(2) Å, respectively. The average bond distance of Mn−L (2.065 Å) is slightly longer than 2.00 Å in agreement with a high spin Mn^{III} species ($S = 2$) [13]. Bond valence sum (BVS) calculation gives the valence sum of 3.067 for manganese in **1** [14]. The result means that the manganese cation in **1** is trivalent clearly. The octahedral coordination sphere of the manganese ion (Mn1) shows an N_4O_2 donor set including one N_{py} (Hpmidip^-), N_{amine} (Hpmidip^-), one O_{alkoxo} (Hpmidip^-), $\text{O}_{\text{hydroxyl}}$ (Hpmidip^-), two nitrogens (azido). The bond angles based on the manganese(III) cation are in the range of 77.09(8) and 175.15(8)°. The coordinated azido ligands are almost linear and exhibit bending modes with the manganese(III) ion (∠N3N4N5; 177.8(3)°, ∠N6N7N8; 176.5(3)°, ∠Mn1N3N4; 121.26(18)°, ∠Mn1N6N7; 121.60(18)°) [15a,b]. The shortest distance of Mn1···Mn1(−x + 1, −y, −z) between the monomeric cations is 4.993 Å. In addition, the oxygen atoms of coordinated Hpmidip^- ligand formed hydrogen bonding interactions [15a,d] with the oxygen atoms of an adjacent monomeric complex each other, which give rise to a supramolecular dimeric structure (O2···O1(−x + 1, −y + 1, −z + 1), 2.623 Å, angle O2−H20···O1 170.76 deg) (Fig. 2).

3.3. Epoxidation reaction catalyzed by manganese catalyst 1 using m-CPBA

Catalytic ability of manganese complex **1** toward olefin epoxidation reaction was identified by using *m*-CPBA (*meta*-chloroperoxybenzoic acid) as an oxidant in solvent (CH_2Cl_2/MeCN, 1:1, 1 mL). Through the control experiments under various conditions, the synergetic effect in epoxidation reaction was confirmed to be terminated within 1 min and to be not affected by the direct reaction of substrate and oxidizing agent. In addition, this complex **1** was robust enough to withstand the oxidation reaction through the UV/Vis spectrophotometry.

The results obtained in the epoxidation reactions of diverse olefin substrates by **1** with *m*-CPBA were summarized in Table 3. In the case of cyclic olefins, like cycloheptene, cyclopentene and cyclooctene, the corresponding products were produced with moderate yields (34.6 to 44.4%, entries 1–3). Besides, cyclohexene gave cyclohexene oxide (49.6%) as a primary product along with trace amount of 2-cyclohexen-1-one (2.7%) and 2-cyclohexen-1-ol (2.1%) as by-products (entry 4). These observations suggest that the free radical reaction of olefin by reactive species was barely involved in the oxidation reaction [6a,16]. Also, 1-hexene and 1-octene, well-known as difficult-to-epoxidize due to the electron deficient environment, were oxidized to the corresponding epoxides with low yields (7.7% and 5.6%, entries 5 and 6) [17]. *cis*-2-Hexene and *cis*-2-octene were used to examine the stereochemistry of the epoxidation reaction. They were mainly oxidized into *cis*-2-hexene oxide and *cis*-2-octene oxide (39.7% and 31.5%, entries 7 and 9) with slight amounts of *trans*-2-hexene oxide and *trans*-2-octene

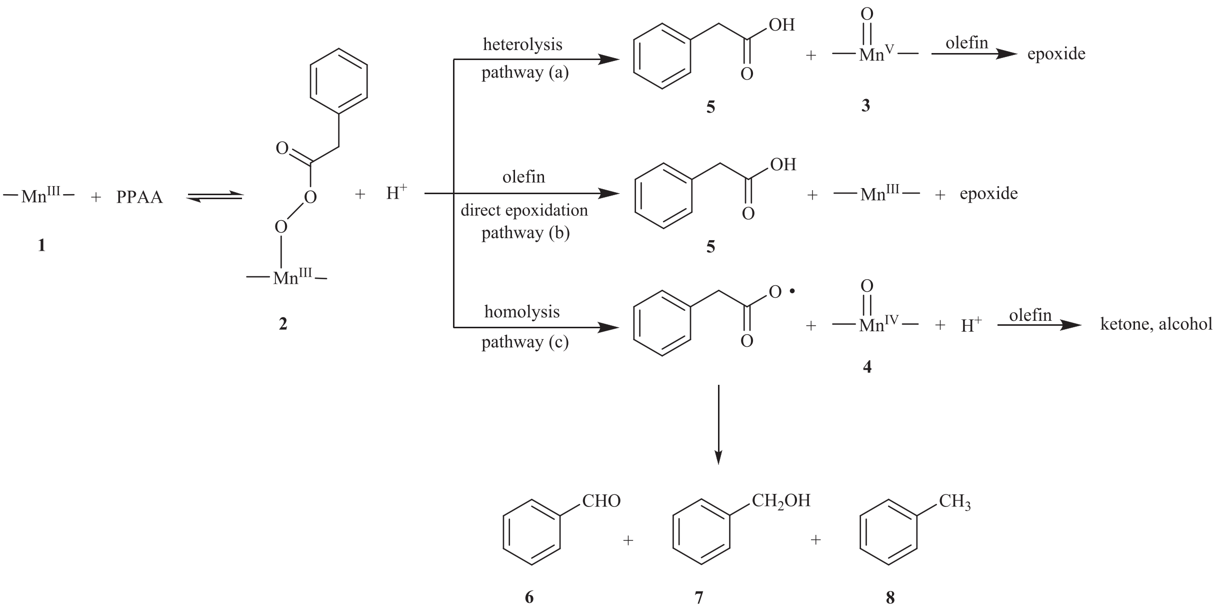

Scheme 1. Plausible degradation pathway of PPAA by manganese catalyst **1**.

Table 4
Product yields derived from PPAA mediated by **1** in the absence and the presence of cyclohexene in CH_2Cl_2/MeCN (1/1).[a]

Entry	Cyclohexene [mM]	Heterolysis[b]	Homolysis[b]			Heterolysis/Homolysis [5/(6 + 7 + 8)]	Oxidation products[c]		
		5	**6**	**7**	**8**		oxide	one	ol
1	0	49.0 ± 3.2	24.5 ± 2.0	1.8 ± 0.1	–	**1.87(65.1/34.9)**	–	–	–
2	20	49.0 ± 1.2	22.7 ± 0.4	1.7 ± 0.1	–	**2.01(66.8/33.2)**	8.7 ± 0.5[d]	1.2 ± 0[d]	0.9 ± 0.1[d]
3	40	58.7 ± 0.2	20.1 ± 0.1	1.4 ± 0.1	–	**2.73(73.2/26.8)**	11.2 ± 0.5[b]	1.3 ± 0[b]	1.1 ± 0[b]
4	80	65.1 ± 0.7	20.6 ± 0.8	1.4 ± 0.1	–	**2.95(74.7/25.3)**	17.1 ± 0.1[b]	1.4 ± 0[b]	1.2 ± 0.2[b]
5	160	71.9 ± 0.3	18.4 ± 0.6	1.3 ± 0	–	**3.65(78.5/21.5)**	27.6 ± 0.6[b]	1.7 ± 0.1[b]	1.8 ± 0.1[b]

[a] Reaction conditions: cyclohexene (0–1.6 × 10^{-1} mmol), catalyst (2.8 × 10^{-3} mmol), PPAA (4 × 10^{-2} mmol), and solvent (1.0 mL, CH_2Cl_2/MeCN = 1:1).
[b] Based on PPAA; **5–8** indicate phenylacetic acid, benzaldehyde, benzyl alcohol, and toluene, respectively.
[c] oxide, -one, and -ol indicate cyclohexene oxide, 2-cyclohexen-1-one, and 2-cyclohexen-1-ol respectively.
[d] Based on the substrate.

Table 5
Product yields derived from PPAA mediated by **1** in the absence and the presence of 1-octene in CH_2Cl_2/MeCN (1/1).[a]

Entry	1-octene [mM]	Heterolysis[b]	Homolysis[b]			Heterolysis/Homolysis [5/(6 + 7 + 8)]	Oxidation products
		5	**6**	**7**	**8**		1-octene oxide
1	0	49.0 ± 3.2	24.5 ± 2.0	1.8 ± 0.1	–	**1.87(65.1/34.9)**	–
2	20	46.4 ± 4.4	18.9 ± 1.8	2.7 ± 0.1	–	**2.14(68.2/31.8)**	–
3	40	49.6 ± 0.4	18.9 ± 0.2	2.4 ± 0.1	–	**2.33(70.0/30.0)**	–
4	80	55.9 ± 4.7	20.0 ± 0.6	2.6 ± 0.1	–	**2.47(71.2/28.8)**	0.4 ± 0.1[c]
5	160	60.0 ± 0	21.6 ± 0.5	2.6 ± 0.1	–	**2.48(71.3/28.7)**	1.8 ± 0[c]

[a] Reaction conditions: 1-octene (0–1.6 × 10^{-1} mmol), catalyst (2.8 × 10^{-3} mmol), PPAA (4 × 10^{-2} mmol), and solvent (1 mL, CH_2Cl_2/MeCN = 1:1).
[b] Based on PPAA; **5–8** indicate phenylacetic acid, benzaldehyde, benzyl alcohol, and toluene, respectively.
[c] Based on the substrate.

Table 6
Competitive epoxidations of *cis*-2-octene and *trans*-2-octene by **1** with *m*-CPBA in MeCN/CH_2Cl_2 (1/1).[a]

Entry	Substrate	Concentration [mM]	Product yield (%)		Ratio of *cis*- to *trans*-oxide
			cis-oxide	*trans*-oxide	
1	*cis*-/*trans*-2-octene	10/10	18.3 ± 1.2[b]	7.6 ± 0.1[b]	**2.4**
2		20/20	15.2 ± 0.6[b]	5.4 ± 0.2[b]	**2.8**
3		40/40	11.7 ± 0.3[c]	4.0 ± 0.2[c]	**2.9**
4		80/80	17.1 ± 0.1[c]	5.0 ± 0.3[c]	**3.4**

[a] Reaction conditions: substrate (0.01–0.08 mmol), catalysts (2.8 × 10^{-3} mmol), and *m*-CPBA (4 × 10^{-2} mmol).
[b] Based on substrate.
[c] Based on *m*-CPBA.

oxide (2.8% and 2.6%, respectively). On the other hand, *trans*-2-hexene and *trans*-2-octene were converted only to *trans*-2-hexene oxide (14.7%, entry 8) and *trans*-2-octene oxide (13.5%, entry 10), respectively. Styrene, aromatic olefin, produced styrene oxide (44.7%, entry 11) as a major product and small amounts of benzaldehyde (2.1%) and phenylacetaldehyde (8.3%). Whereas *cis*-stilbene was converted to *cis*-stilbene oxide (48.3%, entry 12) and trace amount of *trans*-stilbene oxide (5.5%), 2-phenylacetophenone (2.9%) and benzaldehyde (4.6%), *trans*-stilbene produced *trans*-stilbene oxide (37.8%, entry 12) with slight amount of benzaldehyde (4.4%) and 2-pheylacetophenone (8.6%).

Product distribution analysis of these aromatic olefins indicates that either the peroxyl radical or $Mn^{IV}{=}O$ species is somewhat involved in epoxidation reaction as the epoxidizing agent since these species are known to produce radical-induced products [18]. On the other hand, catalytic epoxidation ability of manganese complex **1** is better than those of $[Mn^{II}Cl_2(pypz\text{-}H)_2]$ [5b] and [Mn(bhbda)Cl] [5d].

3.4. Hammett study of competition experiment using para-substituted styrenes and styrene

To examine the electronic character of the reactive intermediates involved in the epoxidation reaction and to consider the effect of substituents on the catalytic reaction rate, we conducted competition experiments using *para*-substituted styrenes and styrene. The Hammett study displayed a ρ value of −1.11, indicating that the electronic

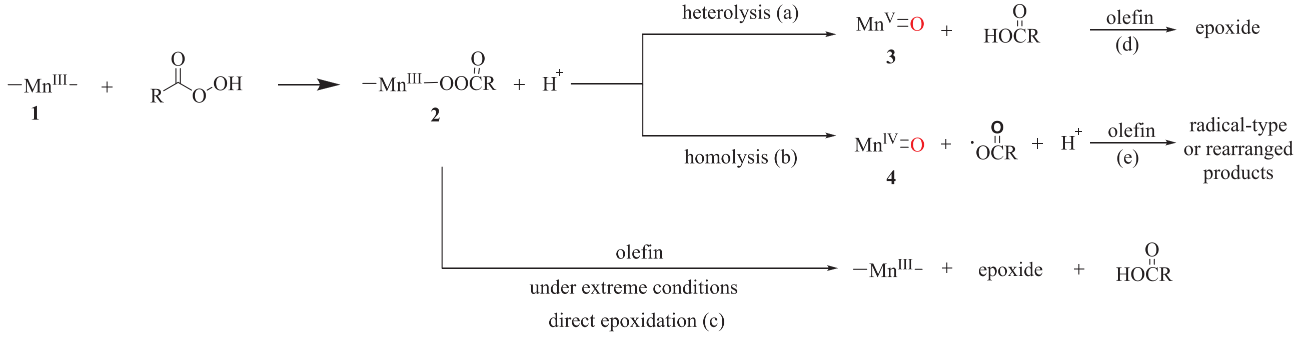

Scheme 2. Possible mechanism for the formation of the reactive intermediates responsible for the olefin epoxidation from the reaction of manganese catalyst **1** with peracid.

character of the reactive intermediates is electrophilic (Fig. 3) [19]. The absolute ρ value obtained with complex **1** is larger than those reported for the epoxidation of *para*-substituent styrenes with $[Mn^{II}(CF_3SO_3)_2(MCP)]$ ($\rho = -0.67$; MCP = *N*,*N*′-dimethyl-*N*,*N*′-bis(2-pyridylmethyl)cyclohexane-*trans*-1,2-diamine) [20], Mn^{III}salen ($\rho = -0.3$) [21], Mn^{III}tetraphenylporphyrin ($\rho = -0.41$) [6b].

3.5. Product distribution of the O—O bond cleavage of PPAA with manganese catalyst 1

The patterns of O—O bond cleavage catalyzed by complex **1** were investigated by using PPAA (peroxyphenylacetic acid), which has been sometimes used as a mechanistic probe. To evaluate the pathway leading to either heterolytic or homolytic cleavage, the degradation products formed from the reaction of PPAA and the catalyst were quantitatively determined [6a,16,22a,23]. Phenylacetic acid (PAA, **5**) is formed through heterolytic cleavage of the O—O bond (pathway (a) of Scheme 1), whereas benzaldehyde (**6**), benzyl alcohol (**7**), and toluene (**8**) are formed via homolytic cleavage (pathway (c)). Also, the direct oxidation reaction of the Mn^{III}—OOC(O)R intermediate (**2**) with substrate produces PAA (pathway (b)) [22].

The results of product distribution of the O—O bond cleavage by the reaction of **1** with PPAA were summarized in Tables 4 and 5. First of all, a control experiment using PPAA as oxidant under the same reaction conditions as used for *m*-CPBA was conducted in the absence of substrate (entry 1 of Tables 4 and 5). Phenylacetic acid as a heterolytic cleavage product (65.0%) and homolytic cleavage products (35.0%) were produced in a ratio of 1.87. The results indicate that the Mn^{III}—OOC(O)R species (**2**) underwent the distribution of heterolysis (65.0%) and homolysis (35.0%) of O—O bond to produce Mn^{V}=O (**3**) and Mn^{IV}=O (**4**), respectively [24]. In the case of easy-to-oxidize substrate, cyclohexene, the increase of substrate concentration (from 0 to 160 mM) caused the ratio of heterolytic to homolytic products to increase from 1.87 (65.1/34.9) to 3.65 (78.5/21.5) (entries 1–5 of Table 4) [6a,22a]. These results suggest that Mn^{III}—OOC(O)R species might be involved in the epoxidation reaction according to the increase of concentration of cyclohexene. In the case of difficult-to-oxidize substrate, 1-octene, the ratio of heterolysis to homolysis increased to less extent from 1.86 (65.0/35.0) to 2.48 (71.3/28.7) (entries 1–5 of Table 5) [6a,23a,23c,24]. These results indicate that the Mn^{III}—OOC(O)R species might be involved to small extent in the epoxidation reaction.

3.6. Competitive reactions of trans-2-octene and cis-2-octene by m-CPBA with manganese complex 1

To get further information about the selectivity of *cis*- and *trans*-2-octene by the active intermediates formed under the catalytic reaction systems, we carried out competition experiments between *cis*-2-octene and *trans*-2-octene. The ratio of *cis*- to *trans*-2-octene oxides increased from 2.4 (18.3/7.6) to 3.4 (17.1/5.0) depending on the increase of the concentration of substrates from 10 to 80 mM, respectively (entries 1–4 of Table 6). In the light of the preference of the Mn^{III}—OOC(O)R species for *cis* over *trans*-olefins due to the steric hindrance between *trans*-type substrate and Mn^{III}—OOC(O)R species, this result indicated that Mn^{III}—OOC(O)R species might be involved to some extent in the epoxidation reactions [25].

3.7. Mechanism

Based on the results obtained in this study, the reasonable mechanism for the olefin epoxidation is proposed in Scheme 2. Peracid as oxidant reacts with catalyst **1** to produce Mn^{III}—OOC(O)R species (**2**) which is divided into Mn^{V}=O (**3**) and Mn^{IV}=O (**4**) species through the heterolytic and homolytic cleavage of O—O bond (pathway (a) and (b) of Scheme 2). The Mn^{V}=O species might be responsible for the production of epoxide and high stereochemical retention, whereas a Mn^{IV}=O species might be ascribed to the radical-type oxidation such as the formation of allylic oxidation products and loss of stereospecificity. Also, under the extreme condition such as high concentration of olefin, Mn^{III}—OOC(O)R species (**2**) would be a probable reactive species for epoxidation (pathway (c)). Finally, the oxidants Mn^{V}=O and Mn^{IV}=O are responsible for epoxidation reaction and radical-type oxidation as key active intermediates, and Mn^{III}—OOC(O)R species has partially participated under the high concentration of olefin substrates.

4. Conclusion

We have prepared and characterized a novel mononuclear manganese species from H_2pmidip and Mn(II) metal ion. The species obtained is a mononuclear manganese(III) complex showing distorted octahedral geometry and is displayed as dimeric structure through O—H···H hydrogen bonding interactions in the solid state. The complex showed selective and effective catalytic activities for olefin epoxidation using *m*-CPBA. To understand the olefin epoxidation reaction, we conducted mechanistic studies such as the Hammett study, the use of PPAA as a mechanistic probe, and competitive experiments of *cis*-2-octene and *trans*-2-octene. Based on the mechanistic studies, the reactive species Mn^{V}=O and Mn^{IV}=O are common reactive oxidants, and Mn^{III}—OOC(O)R intermediate has partially participated to epoxidation reaction under the high concentration of olefin substrates.

Declaration of Competing Interest

The authors declare that they have no known competing financial interests or personal relationships that could have appeared to influence the work reported in this paper.

Acknowledgements

This research was supported by Basic Science Research Program through the National Research Foundation of Korea (NRF) funded by the Ministry of Education, Science and Technology (No. 2018R1D1A1B07043305 and 2018R1A2B6001686). X-ray crystallography at the PLS-II 2D-SMC beamline was supported in part by MEST and POSTECH.

References

[1] (a) K.A. Jørgensen, Chem. Rev. 89 (1989) 431;
(b) P.J. Costa, M.J. Calhorda, F.E. Kühn, Organometallics 29 (2010) 303;
(c) S.A. Hauser, M. Cokoja, F.E. Kühn, Catal. Sci. Technol. 3 (2013) 552;
(d) K. Kamata, K. Yonehara, Y. Sumida, K. Yamaguchi, S. Hikichi, N. Mizuno, Science 300 (2003) 964;
(e) J. Du, C. Miao, C. Xia, Y.-M. Lee, W. Nam, W. Sun, ACS Catal. 8 (2018) 4528.
[2] (a) J.W. Shin, A.R. Jeong, S.Y. Lee, C. Kim, S. Hayami, K.S. Min, Dalton Trans. 45 (2016) 14089;
(b) J.W. Shin, J.M. Bae, C. Kim, K.S. Min, Dalton Trans. 43 (2014) 3999.
[3] A.R. Jeong, J.W. Shin, J.H. Jeong, K.H. Bok, C. Kim, D. Jeong, J. Cho, S. Hayami, K.S. Min, Chem. Eur. J. 23 (2017) 3023.
[4] J.W. Shin, S.R. Rowthu, M.Y. Hyun, Y.J. Song, C. Kim, B.G. Kim, K.S. Min, Dalton Trans. 40 (2011) 5762.
[5] (a) R.V. Ottenbacher, D.G. Samsonenko, E.P. Talsi, K.P. Bryliakov, ACS Catal. 4 (2014) 1599;
(b) E. Manrique, A. Poater, X. Fontrodona, M. Solà, M. Rodríguez, I. Romero, Dalton Trans. 44 (2015) 17529;
(c) S. Kim, K.-B. Cho, Y.-M. Lee, J. Chen, S. Fukuzumi, W. Nam, J. Am. Chem. Soc. 138 (2016) 10654;
(d) M. Sankaralingam, M. Palaniandavar, Dalton Trans. 43 (2014) 538;
(e) L. Gómez, I. Garcia-Bosch, A. Company, X. Sala, X. Fontrodona, X. Ribas, M. Costas, Dalton Trans. (2007) 5539;
(f) V. Abbasi, H. Hosseini-Monfared, S.M. Hosseini, New J. Chem. 41 (2017) 9866.
[6] (a) S.H. Lee, J.H. Han, H. Kwak, S.J. Lee, E.Y. Lee, H.J. Kim, J.H. Lee, C. Bae, S.N. Lee, Y. Kim, C. Kim, Chem. Eur. J. 13 (2007) 9393;
(b) O. Bortolini, B. Meunier, J. Chem. Soc. Perkin Trans. 2 (1984) 1967.
[7] (a) J.H. Han, S.-K. Yoo, J.S. Seo, S.J. Hong, S.K. Kim, C. Kim, Dalton Trans. (2005) 402;
(b) R.A. Sheldon, J.K. Kochi, Metal-Catalyzed Oxidations of Organic Compounds, Academic Press, New York, 1981 ch. 2.
[8] A.J. Arvai, C. Nielsen, ADSC Quantum-210 ADX Program, Area Detector System

Corporation, Poway, CA, USA, 1983.

[9] Z. Otwinowski, W. Minor, Methods in Enzymology, ed. C. W. Carter Jr., R. M. Sweet, Academic Press, New York, 1997, Vol. 276, part A, p. 307.

[10] G.M. Sheldrick, Acta Crystallogr., Sect. A 46 (1990) 467.

[11] G.M. Sheldrick, Acta Crystallogr., Sect. A 64 (2008) 112.

[12] K. Nakamoto, Infrared and Raman Spectra of Inorganic and Coordination Compounds, Part B, 6th ed., John Wiley and Sons, Inc., New Jersey, 2009, pp. 120–131.

[13] (a) G. Aromí, M.J. Knapp, J.-P. Claude, J.C. Huffman, D.N. Hendrickson, G. Christou, J. Am. Chem. Soc. 121 (1999) 5489;
(b) B. Albela, R. Carina, C. Policar, S. Poussereau, J. Cano, J. Guilhem, L. Tchertanov, G. Blondin, M. Delroisse, J.-J. Girerd, Inorg. Chem. 44 (2005) 6959.

[14] (a) W. Liu, H.H. Thorp, Inorg. Chem. 32 (1993) 4102;
(b) I.D. Brown, D. Altermatt, Acta Cryst. B 41 (1985) 244;
(c) N.E. Brese, M. O'Keeffe, Acta Cryst. B 47 (1991) 192;
(d) R.M. Wood, K.A. Abboud, R.C. Palenik, G.J. Palenik, Inorg. Chem. 39 (2000) 2065;
(e) J. Zachara, Inorg. Chem. 46 (2007) 9760.

[15] (a) K.C. Mondal, M.G.B. Drew, P.S. Mukherjee, Inorg. Chem. 46 (2007) 5625;
(b) S. Dalai, P.S. Mukherjee, E. Zangrando, N.R. Chaudhuri, New J. Chem. 26 (2002) 1185;
(c) E.A. Archer, A.E. Sochia, M.J. Krische, Chem. Eur. J. 7 (2001) 2059;
(d) A. Langenstroer, Y. Dorca, K.K. Kartha, M.J. Mayoral, V. Stepanenko, G. Fernández, L. Sánchez, Macromol. Rapid Commun. 39 (2018) 1800191.

[16] (a) T.K.M. Shing, Y.Y. Yeung, P.L. Su, Org. Lett. 8 (2006) 3149;
(b) B. Qiu, D. Xu, Q. Sun, C. Miao, Y.M. Lee, X.X. Li, W. Nam, W. Sun, ACS Catal. 8 (2018) 2479.

[17] (a) I. Garcia-Bosch, X. Ribas, M. Costas, Adv. Synth. Catal. 351 (2009) 348;
(b) M.C. White, A.G. Doyle, E.N. Jacobsen, J. Am. Chem. Soc. 123 (2001) 7194;
(c) A. Murphy, A. Pace, T.D.P. Stack, Org. Lett. 6 (2004) 3119;
(d) K. Sato, M. Aoki, M. Ogawa, T. Hashimoto, R. Noyori, J. Org. Chem. 61 (1996) 8310;
(e) G. Olivo, O. Cusso, M. Borrell, M. Costas, J. Biol. Inorg. Chem. 22 (2017) 425;
(f) E. Hao, Z. Wang, L. Jiao, S. Wang, Dalton Trans. 39 (2010) 2660;
(g) A. Murphy, G. Dubois, T.D.P. Stack, J. Am. Chem. Soc. 125 (2003) 5250;
(h) E. Hao, Z. Wang, L. Jiao, S. Wang, Dalton Trans. 39 (2010) 2660;
(i) R. Ottenbacher, E. Talsi, K. Bryliakov, Catal. Today 278 (2016) 30.

[18] (a) A.M. Al-Ajlouni, J.H. Espenson, J. Am. Chem. Soc. 117 (1995) 9243;
(b) T. Taguchi, K.L. Stone, R. Gupta, K.-L. Benedikt, J. Yama, M.P. Hendrich, A.S. Borovik, Chem. Sci. 5 (2014) 3064;
(c) H.M. Ahn, J.M. Bae, M.J. Kim, K.H. Bok, H.Y. Jeong, S.J. Lee, C. Kim, Chem. Eur. J. 23 (2017) 11969;
(d) A. Guha, D. Das, Indian J. Chem. 50 (2011) 1574;
(e) X. Huang, T. Zhuang, P. Kates, H. Gao, X. Chen, J.T. Groves, J. Am. Chem. Soc. 139 (2017) 15407.

[19] (a) R. Nasrollahi, S. Zakavi, Eur. J. Inorg. Chem. 13 (2017) 2002;
(g) J. Du, C. Miao, C. Xia, T.M. Lee, W. Nam, W. Sun, ACS Catal. 8 (2018) 4528.

[20] I. Garcia-Bosch, A. Company, X. Fontrodona, X. Ribas, M. Costas, Org. Lett. 10 (2008) 2095.

[21] W. Adam, C. Mock-Knoblauch, C.R. Saha-Moller, M. Herderich, J. Am. Chem. Soc. 122 (2000) 9685.

[22] (a) S.H. Lee, L. Xu, B.K. Park, Y.V. Mironov, S.H. Kim, Y.J. Song, C. Kim, Y. Kim, S.-J. Kim, Chem. Eur. J. 16 (2010) 4678;
(b) J.M. Bae, M.M. Lee, S.A. Lee, S.Y. Lee, K.H. Bok, J. Kim, C. Kim, Inorg. Chim. Acta 451 (2016) 8;
(c) C. Choe, Z. Lv, Y. Wu, Z. Chen, T. Sun, H. Wang, G. Li, G. Yin, Mol. Catal. 438 (2017) 230.

[23] (a) Y.J. Song, M.Y. Hyun, J.H. Lee, H.G. Lee, J.H. Kim, S.P. Jang, J.Y. Noh, Y. Kim, S.J. Kim, S.J. Lee, C. Kim, Chem. Eur. J. 18 (2012) 6094;
(b) T.G. Traylor, S. Tsuchiya, Y.S. Byun, C. Kim, J. Am. Chem. Soc. 115 (1993) 2775;
(c) Y.J. Song, S.H. Lee, H.M. Park, S.H. Kim, H.G. Goo, G.H. Eoom, J.H. Lee, M.S. Lah, Y. Kim, S.-J. Kim, J.E. Lee, H.-I. Lee, C. Kim, Chem. Eur. J. 17 (2011) 7336;
(d) W. Nam, H.J. Choi, H.J. Han, S.H. Cho, H.J. Lee, S.Y. Han, Chem. Commun. 25 (1999) 387.

[24] (a) N. Suzuki, T. Higuchi, T. Nagano, J. Am. Chem. Soc. 124 (2002) 9622;
(b) J.T. Groves, Y. Watanabe, Inorg. Chem. 25 (1986) 4808.

[25] (a) T.G. Traylor, F. Xu, J. Am. Chem. Soc. 110 (1988) 1953;
(b) G.-X. He, H.-Y. Mei, T.C. Bruice, J. Am. Chem. Soc. 113 (1991) 5644;
(c) W. Nam, M.H. Lim, H.J. Lee, C. Kim, J. Am. Chem. Soc. 122 (2000) 6641;
(d) B. Wang, Y.-M. Lee, M. Clemancey, M.S. Seo, R. Sarangi, J.-M. Latour, W. Nam, J. Am. Chem. Soc. 138 (2016) 2426;
(e) R. Zhao, J. Wang, D. Zhang, Y. Sun, B. Han, N. Wang, K. Li, Appl. Catal. A Gen. 532 (2017) 26;
(f) M.Y. Hyun, Y.D. Jo, J.H. Lee, H.G. Lee, H.M. Park, I.H. Hwang, K.B. Kim, S.J. Lee, C. Kim, Chem. Eur. J. 19 (2013) 1810;
(g) D. Ostovic, T.C. Bruice, J. Am. Chem. Soc. 110 (1988) 6906;
(h) T.G. Traylor, A.R. Miksztal, J. Am. Chem. Soc. 111 (1989) 7443;
(i) R. Ottenbacher, D. Samsonenko, E. Talsi, K. Bryliakov, ACS Catal. 6 (2016) 979.